(5) S. P. McGlynn, T. Azumi, and M. Kinoshita, "Molecular Spectrscopy of the Triplet State", Prentice-Hall, Englewood Cliffs, N.J., 1969.
(6) E. C. Miller and J. A. Miller in "Chemical Mutagens. Principles and Methods for Their Detection", Vol. I, A. Hollander, Ed., Plenum Press, New York, N.Y., 1971, p 83.
(7) C. C. Irving in "Methods in Cancer Research", Vol. III, H. Busch, Ed., Academic Press, New York, N.Y., 1973, p 189.
(8) J. Elguero, C. Marzin, A. Katritzky, and P. Linda, "The Tautomerism of Heterocycles", Academic Press, New York, N.Y., 1976, Chapter 4.
(9) J. D. Watson and F. H. Crick, *Nature (London)*, **171**, 737, 964 (1953).
(10) P. O. Löwdin, *Biopolymers Symp.*, **1**, 161 (1964).
(11) A. H. Maki and T.-t. Co, *Biochemistry*, **15**, 1229 (1976).
(12) J. Zuclich, J. U. von Schütz, and A. H. Maki, *J. Am. Chem. Soc.*, **96**, 710 (1974).
(13) J. Schmidt, W. S. Veeman, and J. H. van der Waals, *Chem. Phys. Lett.*, **4**, 341 (1969); D. A. Antheunis, J. Schmidt, and J. H. van der Waals, *ibid.*, **6**, 255 (1970); J. Schmidt, D. Antheunis, and J. H. van der Waals, *Mol. Phys.*, **22**, 1 (1971); J. Schmidt, Thesis, University of Leiden, 1971.
(14) J. Zuclich, J. U. von Schütz, and A. H. Maki, *Mol. Phys.*, **28**, 33 (1974); T.-t. Co, R. J. Hoover, and A. H. Maki, *Chem. Phys. Lett.*, **27**, 5 (1974).
(15) A. Albert in "Physical Methods in Heterocyclic Chemistry", Vol. I, A. R. Katritzky, Ed., Academic Press, New York, N.Y., 1963, p 1.
(16) H. C. Börresen, *Acta Chem. Scand.*, **17**, 921 (1963).
(17) J. W. Longworth, R. O. Rahn, and R. G. Shulman, *J. Chem. Phys.*, **45**, 2930 (1966).
(18) E. A. Chandross in "The Exciplex", M. Gordon and W. R. Ware, Ed., Academic Press, New York, N.Y., 1975, p 187.
(19) G. Jackson and G. Porter, *Proc. R. Soc. London, Ser. A*, **260**, 13 (1961).
(20) T. S. Kuan, D. S. Tinti, and M. A. El Sayed, *Chem. Phys. Lett.*, **4**, 507 (1970).
(21) C. B. Harris, D. S. Tinti, M. A. El Sayed, and A. H. Maki, *Chem. Phys. Lett.*, **4**, 409 (1969); M. J. Buckley, C. B. Harris, and A. H. Maiki, *ibid.*, **4**, 591 (1970).
(22) P. Szerenyi and H. H. Dearman, *J. Chem. Phys.*, **58**, 2467 (1973).
(23) T.-t. Co and A. H. Maki, *Biochemistry*, **17**, 182 (1978).
(24) J. W. Sidman, *J. Mol. Spectrosc.*, **2**, 333 (1958); H. F. Hameka and L. J. Oosterhoff, *Mol. Phys.*, **1**, 358 (1958).
(25) J. H. van der Waals and M. S. de Groot in "The Triplet State", A. B. Zahlan, Ed., Cambridge University Press, New York, N.Y., 1967, p 101.
(26) Reference 5, Chapter 9, and references cited therein.
(27) S. A. Boorstein and M. Gouterman, *J. Chem. Phys.*, **39**, 2443 (1963).
(28) Y. Gondo and A. H. Maki, *J. Chem. Phys.*, **50**, 3270 (1969).
(29) J. Zuclich, *J. Chem. Phys.*, **52**, 3592 (1970).
(30) D. S. McClure, *J. Chem. Phys.*, **17**, 665 (1949); **20**, 682 (1952).
(31) B. J. Cohen and L. Goodman, *J. Am. Chem. Soc.*, **87**, 5487 (1965).
(32) E. T. Harrigan and N. Hirota, *J. Am. Chem. Soc.*, **97**, 6647 (1975).
(33) J. Zuclich, *J. Chem. Phys.*, **52**, 3586 (1970).
(34) J. S. Vincent and A. H. Maki, *J. Chem. Phys.*, **39**, 3088 (1963).
(35) C. A. Hutchison, Jr., and B. W. Mangum, *J. Chem. Phys.*, **29**, 952 (1958); **32**, 1261 (1960); **34**, 908 (1961).
(36) E. Kochanski and A. Pullman, *Int. J. Quantum Chem.*, **3**, 1055 (1969); J. P. Daudey and A. Pullman, *Chem. Phys. Lett.*, **5**, 347 (1970).
(37) J. M. Read, Jr., and J. H. Goldstein, *J. Am. Chem. Soc.*, **87**, 3440 (1965).
(38) M.-T. Chenon, R. J. Pugmire, D. M. Grant, R. P. Panzica, and L. B. Townsend, *J. Am. Chem. Soc.*, **97**, 4627, 4636 (1975).
(39) D. G. Watson, R. M. Sweet, and R. E. Marsh, *Acta Crystallogr.*, **19**, 573 (1965).

# Methylmercury as a Spin–Orbit Probe. Effect of Complexing on the Excited State Properties of Tryptophan, Tryptamine, and Benzimidazole

**Peter Svejda, August H. Maki,* and Richard R. Anderson**

*Contribution from the Department of Chemistry, University of California, Davis, California 95616.* *Received April 20, 1978*

**Abstract:** The binding of $CH_3Hg^{II}$ with tryptophan (HTrp), tryptamine ($HTam^+$), and benzimidazole (HBIm) has been observed and formation constants ($K_f$) are reported. $K_f$ for binding at the amine site of HTrp and $HTam^+$ is about 60 and 10 times, respectively, that predicted from the observed correlation of log $K_f$ with the aminium $pK_a$ for a series of simple primary amines. The enhancement is attributed to a specific interaction between $CH_3Hg^{II}$ and the indole ring. NMR chemical shifts point to a location of the methyl group above the indole plane, and model building confirms the possibility of an unstrained geometry with $CH_3Hg^{II}$ located parallel to and in close contact with the aromatic plane. In the complex with HBIm, $CH_3HgHBIm^+$, the NMR chemical shift of $CH_3$ is downfield, consistent with $\sigma$ bonding of $CH_3Hg^{II}$ at N3 of HBIm. $CH_3Hg^{II}$ binding quenches the fluorescence of each compound, and enhances the radiative quantum yield of phosphorescence, that of $CH_3HgTrp$ becoming $0.9 \pm 0.1$. Phosphorescence lifetime measurements at 77 K yield reduction factors of 6000 (HTrp), 8000 ($HTam^+$), and 40 (HBIm) relative to the unperturbed compound. Differences in the magnitude of the heavy atom effect as measured by phosphorescence lifetime reduction are attributed to differences in the position of $CH_3Hg^{II}$ relative to the affected chromophore. Optically detected magnetic resonance measurements, and pulsed laser-excited phosphorescence decay measurements at 1.1–1.2 K show that the heavy atom effect differs for individual triplet sublevels. Complexing of HBIm with $CH_3Hg^{II}$ has the same effect on the triplet state zero-field splittings as does protonation, suggesting that spin–orbit coupling and electron delocalization effects are not important.

## Introduction

Methylmercury is a widely occurring and highly toxic environmental pollutant.[1] The neurotoxicity of $CH_3Hg^{II}$ is well documented,[2] and mutagenic effects also have been observed.[3-6] There has been a continuing interest in the study of $CH_3Hg^{II}$ binding with various bases, and the formation constants of many methylmercury complexes have been determined.[7-15]

We have been interested in the identification of specific base targets and binding sites of alkylmercury in polynucleotides using optical detection of magnetic resonance (ODMR) methods,[16] with which many properties of the phosphorescent state can be uncovered. The mercury atom, which is in effect a spin–orbit probe, induces a heavy atom effect[17] in the target molecule. Binding of the spin–orbit probe leads to fluorescence quenching by enhancement of the intersystem crossing rate, and results in a reduction of the triplet lifetime, frequently accompanied by an increase in the phosphorescence quantum yield.[18] The ODMR sensitivity increases with increasing triplet radiative quantum yield. Magnetic resonance passage conditions also can be made rapid enough to discriminate against signals from long-lived triplet states. We have found in numerous cases that ODMR signals from uncomplexed molecules can be effectively suppressed relative to those complexed with a spin–orbit probe, especially when the latter enhances the phosphorescence quantum yield.[19,20]

During recent ODMR investigations of $CH_3Hg^{II}$ complexes of nucleosides and nucleotides,[20] we added equimolar $CH_3HgOH$ to 1 mM solutions of indole in order to satisfy

0002-7863/78/1500-7138$01.00/0 

ourselves that in a case where no complexing is expected to take place, there will be no observable heavy atom effect at such low concentrations of perturber (i.e., that the external heavy atom effect results from a short-range interaction between the perturber and the affected molecule which must be in mutual contact). As expected, we observed no effect on the phosphorescence lifetime of indole, which remains 6.5 s in the presence of 1 mM $CH_3HgOH$. In a parallel experiment using tryptophan (HTrp), however, we were surprised to observe a striking heavy-atom perturbation of HTrp, whose phosphorescence lifetime was reduced from the unperturbed 6.5 s to about 1 ms. Although $CH_3Hg^{II}$ binding to the amino and carboxylate groups of amino acids has been observed,[15] the extent of the triplet lifetime shortening was unexpected based upon the number of atoms intervening between the indole chromophore and the heavy-atom perturber.

In this communication we report the results of a more thorough investigation of the methylmercury-tryptophan complex ($CH_3HgTrp$) by ODMR as well as by other spectroscopic methods including high-resolution NMR. Parallel investigations of $CH_3HgOH$ complexing with tryptamine ($HTam^+$) and benzimidazole (HBIm) are reported, as well. Formation constants are reported and compared with those of other amines. Based upon these measurements, we propose rather specific conformational models for $CH_3HgTrp$, $CH_3HgTam^+$, and the benzimidazole complex, $CH_3HgHBIm^+$.

## Experimental Section

L-Tryptophan (Calbiochem, Inc., A grade, chromatographically homogeneous) and tryptamine (Fluka, Inc., puriss.) were found to be free of luminescent impurities, and were used without treatment. Benzimidazole (Eastman, Inc.) was recrystallized from deionized, doubly distilled water; the product was stored in total darkness, and handled only under conditions of subdued lighting. Methylmercury hydroxide (Alfa Products, Inc., 97%) was dissolved in deionized, doubly distilled water, and the stock solution was standardized by the method of Waugh et al.[21] Ethylene glycol (EG) was Matheson Coleman and Bell, Inc., Chromatoquality, which was found to be effectively free of luminescent impurities when used from a freshly opened container. For phosphorescence and ODMR measurements, the concentrations of HTrp, $HTam^+$, and HBIm were 1 mM in 50:50 (v/v) EG-water. The pH was measured at 24 °C with a pH meter employing a glass electrode (Beckman, Inc., Model 4500). The effective pH measured in this manner is referred to as pH*. The pH* of solutions in the range 5–7 was maintained with 0.1 M phosphate buffer. At lower pH*, $H_3PO_4$ was used, while at higher pH*, NaOH was used to adjust pH*.

Phosphorescence decay measurements of $HBIm-CH_3Hg^{II}$ complexes were signal averaged and deconvoluted by computer as described previously.[22] The phosphorescence lifetime of the $CH_3HgTrp$ and $CH_3HgTam^+$ complexes proved to be too short to measure using this procedure[22] because of the 1.5-ms response time of the shutters. Excitation was carried out with a pulsed dye laser (Chromatix, Inc., Model CMX-4, pulse width ca. 2 μs). Excitation was at 296 nm, obtained by second harmonic generation from the Rhodamine 6G fundamental, which was suppressed by a CS 7-54 glass filter (Corning, Inc). The photomultiplier output passed through a homemade source follower with a constant gain of 10 and a minimum band width of 15 MHz. The signal was applied next to a fast digitizing transient recorder (Biomation, Inc., Model 610B) interfaced with a 1024 channel multichannel analyzer (Nicolet, Inc., Model 1072) and subsequent deconvolution was carried out as described previously.[22] Microwave induced delayed phosphorescence (MIDP)[23] measurements were made in a manner similar to the phosphorescence decays;[22] excitation was with a high-pressure mercury arc (Orsam, Inc., HBO-100) filtered with a water filter, a 0.25-m monochromator (Bausch and Lomb, Inc., No. 33-86-75) set for ca. 8 nm band-pass, and a CS 7-54 glass filter. A rapid microwave frequency sweep through a zero-field magnetic resonance was applied after a variable time delay following the closing of an excitation shutter and the simultaneous opening of a shutter in the monitoring path (shutter response time ca. 1.5 ms).

Slow-passage ODMR measurements were made according to previously described procedures.[22,24] Microwave-induced phosphorescence transient signals[25] were measured on some samples. Total luminescence spectra were measured at 77 K with a Perkin-Elmer, Inc., MPF-2A spectrofluorimeter.

Formation constants of the methylmercury complexes were measured at ambient temperature (23–24 °C) on a Varian, Inc., Cary Model 17 spectrophotometer using an absorbance difference method. Samples were measured in matched 1-cm cells at concentrations in the range $10^{-5}$–$10^{-4}$ M. The sample compartment and the reference compartment each were fitted with two cells, one containing the buffered sample, the other pure buffer. The concentrated $CH_3HgOH$ stock solution was added from a microliter syringe in equal increments to the sample-containing cell of the sample compartment and the buffer-containing cell of the reference compartment. An equal volume of buffer was added to the sample-containing cell of the reference compartment to compensate for differential sample dilution. Each cell was stirred thoroughly with its own glass stirrer after each addition; the stirrers were stored with their clinging liquid for the next incremental addition. A difference spectrum was run before and after each addition of $CH_3HgOH$ over a sufficient wavelength range to verify the continued presence of two or more isosbestic points. The total dilution of the sample was never more than 5% during a run, and was frequently 1% or less; the intensity of the monitored difference peak was corrected for this dilution. The treatment of the data is discussed in the following section.

Chemical shifts and $^{199}Hg-^1H$ spin-spin coupling constants of the methyl protons of $CH_3Hg^{II}$ were measured at 100 MHz with a JEOL, Inc., EC-100 Fourier transform NMR spectrometer supplied with a Texas Instruments, Inc., 908A data system. Samples were dissolved in 99.8% $D_2O$, and the shifts were related to the residual HDO proton peak. A 180°-$\tau$-90° pulse sequence was used with $\tau$ selected (~3 s) to minimize the amplitude of the HOD peak. Observed chemical shifts and spin-spin coupling constants were corrected for the partitioning of $CH_3Hg^{II}$ between various species using known values of the appropriate equilibrium constants.

## Results

The formation constants of the methylmercury complexes studied in this work are defined in terms of the equilibrium

$$CH_3HgOH + HB \rightleftharpoons CH_3HgB + H_2O,$$
$$K_f = [CH_3HgB]/[CH_3HgOH][HB] \quad (1)$$

HB represents the tryptophan zwitterion (HTrp), the cation of tryptamine ($HTam^+$) or that of benzimidazole ($H_2BIm^+$). The methylmercury binding with HTrp and $HTam^+$ was studied in pH 8 phosphate buffer; the dominant uncomplexed amine species at this pH are HTrp and $HTam^+$, respectively. Minor species were neglected in the analysis. Unbound methylmercury is effectively all undissociated hydroxide.[7,14,15] Furthermore, free $CH_3HgOH$ concentrations above $5 \times 10^{-4}$ M did not occur in our $K_f$ determinations, so that the higher complexes, $(CH_3Hg)_2OH^+$ and $(CH_3Hg)_3O^+$, are completely negligible.[14,26] Equation 1, therefore, represents the major species present in these solutions, and others were neglected in the analysis. The following equation, which is derived readily assuming 1:1 complex formation, was found to be convenient for the analysis of the absorption difference data:

$$G = \Delta A_\infty^{-1} + (K_f^{-1} + c_0)\Delta A_\infty^{-1} c_h^{-1} \quad (2a)$$

where

$$G = \Delta A^{-1} + \Delta A_\infty^{-2} c_0 c_h^{-1} \quad (2b)$$

In eq 2, $\Delta A$ is the absorbance difference at the wavelength of measurement, $\Delta A_\infty$ is the limiting absorbance difference corresponding to complete complex formation, $c_0$ is the total concentration of amine, and $c_h$ is the total concentration of added methylmercury. A difference peak at 229 nm was used for the analysis of both HTrp and $HTam^+$. Isosbestic points were found to occur at 224.5, 249.5, 280, and 287.5 nm for HTrp, and at 223.5, 259, 279, and 288 nm for $HTam^+$. Equation 2a was fit to the experimental data for a run by

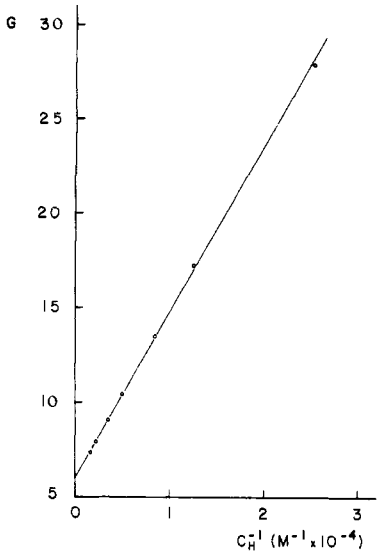


**Figure 1.** $G$ vs. $c_h^{-1}$ for methylmercury binding with tryptophan. $\Delta A$ measured at 229 nm, $c_0 = 3.0 \times 10^{-5}$ M in 0.02 M pH 8 phosphate buffer. Quantities are defined in eq 2.

successive approximations beginning with neglect of the second term on the right-hand side of eq 2b. A first approximation for $\Delta A_\infty$ was obtained from the intercept of a weighted least-squares linear regression of $A^{-1}$ vs. $c_h^{-1}$. Weighting of the points were proportional to $\Delta A^2$. $G$ was calculated for each point using this approximation for $\Delta A_\infty$ and the weighted least-squares regression of $G$ vs. $c_h^{-1}$ was repeated until a constant value of $\Delta A_\infty$ was obtained. $K_f$ was obtained from the slope and intercept of the final regression. Once $\Delta A_\infty$ was obtained, the data also were checked using eq 3, which should hold for 1:1 complex formation.

$$-\log (\Delta A^{-1} - \Delta A_\infty{}^{-1}) = \log K_f + \log (c_h \Delta A_\infty - c_0 \Delta A) \quad (3)$$

A plot of $-\log (\Delta A^{-1} - \Delta A_\infty{}^{-1})$ vs. $\log (c_h \Delta A_\infty - c_0 \Delta A)$ is linear for the measurements of binding to HTrp and to $HTam^+$ with a least-squares slope of 1.005 and 1.001, respectively, for typical runs. Log $K_f$ obtained from the intercept is in excellent agreement with that obtained from eq 2.

No isosbestic points were found to HBIm complexing with $CH_3HgOH$ at pH 8. It was concluded that more than one complex was being formed simultaneously at this pH, i.e.,

$$HBIm + CH_3HgOH \rightleftharpoons CH_3HgHBIm^+ + OH^- \rightleftharpoons CH_3HgBIm + H_2O \quad (4)$$

$$CH_3HgHBIm^+ + CH_3HgOH \rightleftharpoons (CH_3Hg)_2BIm^+ + H_2O \quad (5)$$

Similar pH-dependent equilibria occur in the complexing of $CH_3HgOH$ with imidazole.[27] When the pH was reduced to 6, the difference spectra showed isosbestic points at 270.2, 273.0, and 276.3 nm. Positive and negative difference peaks at 274.6 and 277.9 nm, respectively, were chosen for analysis using eq 2. The data fit eq 3, and yielded a least-squares slope of 1.002. The equilibrium constant given by this procedure is not $K_f$, defined according to eq 1, since the major free amine species is not $H_2BIm^+$ at pH 6, but rather HBIm. Also, about 3% of the free methylmercury is present as $CH_3Hg^+$. Correction of the apparent formation constant at pH 6 was made using $pK_a = 5.53$[28] for $H_2BIm^+$, and $K = 3.2 \times 10^{-10}$ for the dissociation

$$CH_3HgOH \rightleftharpoons CH_3Hg^+ + OH^-$$ [7]

A typical plot of eq 2 using data for HTrp binding is shown in Figure 1. The $K_f$ are given in Table I along with $K_f$ determined for other amines by Rabenstein et al.[15] using $^1H$ NMR.

**Table I.** Aminium Ionization Constants and Formation Constants of Methylmercury Amine Complexes

| amine | $pK_a$[a] | log $K_f$[b] |
|---|---|---|
| ammonia | 9.32 | 2.42[c] |
| methylamine | 10.81 | 1.23[c] |
| ethylamine | 10.82 | 1.31[c] |
| isopropylamine | 10.76 | 1.29[c] |
| β-aminopropionic acid | 10.25 | 1.80[d] |
| *tert*-butylamine | 10.81 | 1.20[c] |
| glycine | 9.69 | 2.67[d] |
| valine | 9.81 | 2.09[d] |
| phenylalanine | 9.13[e] | 3.64[d] |
| tryptophan | 9.39[e] | 3.92[f,g] |
| | | 4.18[f,h] |
| tryptamine | 10.2[i] | 2.36[f,j] |
| | | 2.69[f,g] |
| | | 2.87[f,h] |
| benzimidazole | 5.53[k] | 4.34[f,l] |

[a] Refers to $HB^+ \rightleftharpoons B + H^+$. Values from ref 15 unless otherwise indicated. [b] Refers to $HB^+ + CH_3HgOH \rightleftharpoons CH_3HgB^+ + H_2O$. Values calculated from ref 15 unless otherwise indicated. HTrp, $HTam^+$, and HBIm data are at 24 °C. [c] Ionic strength ($I$) = 0.4–0.6 M. [d] $I$ = 0.2–0.3 M. [e] G. M. Barenboim, A. N. Domanskii, and K. K. Turoverov, "Luminescence of Biopolymers and Cells", Plenum Press, New York, N.Y., 1969. [f] This work. Estimated accuracy, ±0.04. [g] pH 8, 0.02 M phosphate buffer. [h] pH 8, 0.005 M phosphate buffer. [i] D. D. Perrin, "Dissociation Constants of Organic Bases in Aqueous Solution", Butterworths, London, 1965, p 239. [j] pH 8, 0.04 M phosphate buffer. [k] Reference 28. [l] pH 6, 0.02 M phosphate buffer.

Addition of a five-fold molar excess of $CH_3HgOH$ to a $10^{-3}$ M HTrp solution at pH 7 in EG-water results in nearly complete quenching of the fluorescence, and enhancement of the phosphorescence intensity at 77 K. Based upon previous quantum yield measurements,[29] we can estimate that the unperturbed phosphorescence quantum yield ($\phi_p = 0.17$) increases to $\phi_p = 0.9 \pm 0.1$ upon complexing with methylmercury. The luminescence of indole under the same conditions is unaffected, so we can infer that complexing occurs with HTrp and that the binding site involves the α-amino acid side chain—most likely the amine nitrogen. It has been shown[15] that $CH_3Hg^+$ binding to carboxylate in amino acids becomes predominant only at low pH. A similar heavy atom effect is observed when the measurements are repeated using $HTam^+$ or HBIm in place of HTrp. A comparison of the luminescence spectra of HTrp and $CH_3HgTrp$ is shown in Figure 2. The structure of the phosphorescence is not greatly affected by complex formation, although a red shift of the 0-0 peak by ca. 4 nm is observed. As the pH is lowered, the fluorescence quenching becomes less complete indicating competition by the proton for the amine binding site. In the case of $CH_3HgOH$ binding to $HTam^+$, there is even a smaller red shift of the phosphorescence 0-0 peak (ca. 1.3 nm). Chen[30] has observed a heavy-atom effect upon addition of $Ag^+$ to HTrp which results in the quenching of fluorescence. With $Ag^+$, the spectral characteristics of the phosphorescence change markedly; there is a loss of vibrational structure, and the band is markedly red shifted for $Ag^+/HTrp \geq 5$.

The phosphorescence spectra of HBIm and its 1:1 complex with $CH_3Hg^+$ ($CH_3HgHBIm^+$) are compared in Figure 3. The spectrum is not greatly affected by complex formation. A blue shift of the 0-0 band maximum of 1.5 nm occurs which is comparable to the small blue shift (2.1 nm) which is observed upon protonation.[31] The 0-0 band peak positions and the phosphorescence decay rate constants measured at 77 K for the amines and their complexes are given in Table II. A red

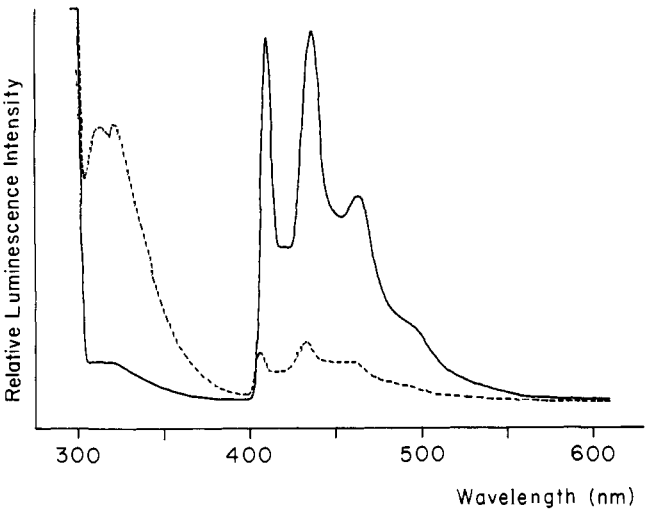


**Figure 2.** Luminescence spectra of tryptophan (- - -) and its complex with methylmercury (—) at 77 K. Solvent is 1:1 EG-$H_2O$, pH* 7. Excitation is at 290 nm, and spectra are not corrected for spectrometer response. Spectra are taken at comparable spectrometer sensitivities.

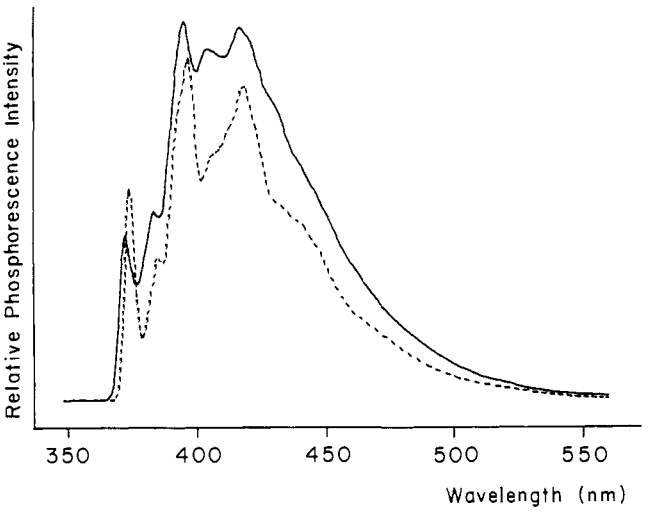


**Figure 3.** Phosphorescence spectra of benzimidazole, pH* 11.2 (- - -), and its 1:1 complex with methylmercury, pH* 5 (—), at 1.1 K. Solvent is 1:1 EG-$H_2O$, and spectra are uncorrected for spectrometer response. Excitation is at 280 nm. Spectrometer sensitivity is reduced for the methylmercury complex spectrum.

**Table II.** Phosphorescence Decay Constants of Tryptophan, Tryptamine, Benzimidazole, and Their Methylmercury Complexes at 77 K

| compd[a] | pH*[b] | $R$[c] | $\lambda P_{0-0}$, nm[d] | $\bar{k}$, $s^{-1}$[e] |
|---|---|---|---|---|
| tryptophan | 7. | 0.0 | 405.7 | 0.15[f] |
| | 7. | 5. | 409.8 | 910. |
| tryptamine | 8. | 0.0 | 406.8 | 0.15[f] |
| | 8. | 5. | 408.2 | 1190. |
| benzimidazole | 11.2[g] | 0.0 | 373.5 | 0.16[f] |
| | 1.3[h] | 0.0 | 371.4 | 0.16[f] |
| | 5. | 0.9 | 372.0 | 6.6 |
| | 6. | 1.2 | *i* | 5.9 |
| | 7. | 5. | 372.5 | 11.1 |
| | 8.5 | 10. | 373.1 | 11.7 |

[a] 1 mM in 50:50 (v/v) EG-$H_2O$. $\lambda_{exc}$ = 280-290 nm. [b] Apparent pH of solution at 24 °C measured with glass electrode. Solutions with 6 ≤ pH* ≤ 8 contained 0.1 M phosphate buffer. Other pH* obtained with $H_3PO_4$ or NaOH. [c] Concentration (mM) of added $CH_3HgOH$. [d] Peak wavelength of phosphorescence 0-0 band (calibrated using low-pressure Hg discharge) and wavelength at which phosphorescence was monitored. [e] Average decay constant; see text. Decay is nonexponential except as noted. [f] Exponential decay. [g] Neutral molecule. [h] Protonated cation. [i] Not measured accurately.

shift (1.1 nm) of the 0-0 peak of the HBIm phosphorescence at $CH_3HgOH$/HBIm ($R$) = 10, pH 8.5, relative to $R$ = 0.9, pH 5, and a shorter triplet lifetime under the former conditions provide evidence that the 2:1 complex, $(CH_3Hg)_2BIm^+$, is formed. Except for HTrp, $HTam^+$, HBIm, and $H_2BIm^+$, the decays are nonexponential. The nonexponential decays were deconvoluted, and the weighted average of the resulting decay constants is reported. An exponential component was weighted by the preexponential factor obtained in the decay deconvolution. We believe that the nonexponential decay behavior represents a more or less continuous distribution of decay lifetimes present in the sample, rather than the presence of different complexes with discrete lifetimes. The triplet lifetimes of the uncomplexed amines are long and nearly the same. Complexing with $CH_3Hg^{II}$ reduces the triplet lifetimes of HTrp and $HTam^+$ by a factor of 6000-8000; complexing with one $CH_3Hg^+$ reduces the lifetime of HBIm about 40 times, while the 2:1 complex appears to have a lifetime about 70 times shorter than that of HBIm. Surprisingly, the external heavy atom effect as measured by the triplet lifetime is over two orders of magnitude larger in the case of HTrp and $HTam^+$ than it is for HBIm, even though the Hg atom in the latter is bound directly to the imidazole nitrogen atom of the chromophore. The interaction of the heavy atom with the aromatic chromophore clearly is different in HTrp and $HTam^+$ than it is in HBIm. Evidence from NMR measurements which relates to the structure of these complexes will be presented later in this section.

The results of ODMR slow-passage measurements on HTrp, $HTam^+$, HBIm, $H_2BIm^+$, and their methylmercury complexes are listed in Table III. It is apparent that complexing with $CH_3Hg^{II}$ has a significant effect upon the zero-field ODMR frequencies of HTrp and $HTam^+$. The frequencies $\nu_1$ and $\nu_2$ correspond to the $(D - |E|)$ and $2|E|$ transitions, respectively, in HTrp;[32,33] we will assume the same assignment for $HTam^+$ by analogy. The major axis of the zero field splitting (ZFS) tensor corresponding to $D$ is normal to the plane of the indole ring. The assignment of $D$ and $|E|$ for $CH_3HgTrp$ depends upon whether or not the $\nu_1$ and $\nu_2$ transitions have crossed each other in frequency. The two likely assignments of $D$ and $|E|$ are given in Table III. Complexing with $CH_3Hg^{II}$ causes an increase in the magnitude of $D$ and a decrease in that of $|E|$ in the case of either assignment of $\nu_1$ and $\nu_2$. The perturbation of the ZFS caused by $CH_3Hg^{II}$ complexing with $HTam^+$ is greater than in the case of HTrp. The $\nu_1$ and $\nu_2$ resonances now are well resolved, but again we cannot be sure of the assignment of these transitions, since $\nu_1$ and $\nu_2$ may or may not have crossed in the complex. Both likely assignments, $D > 3|E|$ and $D < 3|E|$, are included in Table III. For either assignment, $D$ increases upon complexing with $CH_3Hg^{II}$. Formation of the complex $CH_3HgHBIm^+$ at $R$ = 0.9, pH 5 leads to large changes of the $\nu_i$ from the values found for HBIm. The effect of methylmercuration on the ZFS of HBIm is virtually identical, however, with that caused by protonation.[31] Furthermore, the binding of a second $CH_3Hg^{II}$ ($R$ = 10, pH 8.5) results in no further change in the ZFS. The effects of $CH_3Hg^+$ binding to HBIm on the ZFS of the triplet state appear to be mainly electrostatic (rather than involving electron delocalization or spin-orbit coupling) since they are mimicked so well by protonation.

An estimate of the individual sublevel decay constants was obtained by the MIDP method,[23] with measurements made at the lowest temperature available in our apparatus, 1.1-1.2 K, in order to minimize the effects of spin-lattice relaxation.

**Table III.** ODMR Frequencies and ZFS Parameters of Tryptophan, Tryptamine, Benzimidazole, and Their Methylmercury Complexes[a]

| compd | $\nu_1$ ($\Delta\nu$)[b] | $\nu_2$ ($\Delta\nu$)[b] | $\nu_3$ ($\Delta\nu$)[b] | $D$, $m^{-1}$ [c] | $\lvert E\rvert$, $m^{-1}$ [c] |
|---|---|---|---|---|---|
| HTrp[d] | 1.74 (165) | 2.45 (345) | | 9.88 | 4.08 |
| $CH_3HgTrp$ | 1.97 (200) | 2.17 (340) | 4.23 (270) | 10.48 | 3.62 |
| | | | | 10.82 | 3.28 |
| $HTam^+$ | 1.74 (110) | 2.46 (260) | 4.22 (150)[e] | 9.94 | 4.10 |
| $CH_3HgTam^+$ | 1.58 (140) | 3.32 (290) | 5.1 (1700) | 10.8 | 5.54 |
| | | | | 13.7 | 2.64 |
| HBIm[f] | 1.95 (490) | 2.58 (310) | 4.31 (790) | 11.50 | 3.25 |
| $H_2BIm^+$ [f] | 0.79 (90) | 3.18 (120) | 3.90 (100) | 11.80 | 1.32 |
| $CH_3HgHBIm^+$ [g] | 0.71 (108) | 3.27 (60) | 3.91 (100) | 11.97 | 1.18 |
| $(CH_3Hg)_2BIm^+$ [h] | 0.72 (115) | 3.28 (59) | 3.91 (100) | 11.99 | 1.20 |
| $(CH_3Hg)_2BIm^+$ [i] | 0.72 (110) | 3.24 (63) | 3.88 (85) | 11.87 | 1.20 |

[a] Conditions as in Table II, except $T$ = 1.1–1.2 K. [b] Observed peak ODMR frequencies (GHz); numbers in parentheses are signal widths (fwhm) (MHz). [c] ZFS parameters; see text for axis system assignment. When two sets of values are given, assignment is in doubt. [d] References 24, 32, and 33. [e] Observed via EEDOR, only. [f] Data from ref 31, in which assignments are given. [g] pH* 5, $R$ = 0.9. [h] pH* 7, $R$ = 5. [i] pH* 8.5, $R$ = 10.

**Table IV.** Apparent Triplet Sublevel Decay Constants of Methylmercury Complexes of Tryptophan, Tryptamine, and Benzimidazole

| complex[a] | $R$ | pH* | $\kappa_1$, $s^{-1}$ [b] | $\kappa_2$, $s^{-1}$ [b] | $\kappa_3$, $s^{-1}$ [b] | $\bar{\kappa}$, $s^{-1}$ [c] |
|---|---|---|---|---|---|---|
| $CH_3HgTrp$ | 5. | 7. | 21. ($\nu_1$,[d] $\nu_2$, $\nu_3$) | 240. ($\nu_2$) | 2600.[e] | 960. |
| $CH_3HgTam^+$ | 5. | 8. | 30. ($\nu_1$,[d] $\nu_2$, $\nu_3$) | 2100.[f] | 2100.[f] | 1410. |
| $CH_3HgHBIm^+$ | 0.9 | 5. | 2.3 ($\nu_2$, $\nu_3$) | 8.3 ($\nu_2$) | 11.6 ($\nu_3$) | 7.4 |
| $(CH_3Hg)_2BIm^+$[g] | 5. | 7. | 2.3 ($\nu_2$, $\nu_3$) | 11.5 ($\nu_2$) | 16.2 ($\nu_3$) | 10.0 |
| | 10. | 8.5 | 2.5 ($\nu_2$, $\nu_3$) | 15.1 ($\nu_2$) | 18.7 ($\nu_3$) | 12.1 |

[a] Conditions as in Table III. $\kappa_i$ from MIDP measurements unless otherwise indicated. [b] Apparent sublevel decay constant, arranged in order of increasing $\kappa_i$. Parentheses indicate which ODMR frequencies (Table III) produced response with observed $\kappa_i$. If produced by more than one $\nu_i$, indicated $\kappa_i$ is the average. [c] $(\kappa_1 + \kappa_2 + \kappa_3)/3$. [d] Weak response. [e] From deconvolution of pulse laser excited phosphorescence decay at 1.1 K, fixing $\kappa_1$ and $\kappa_2$ in the analysis. [f] From deconvolution of laser-excited decay at 1.1 K fixing $\kappa_1$ in analysis. Value is average of $\kappa_2$ and $\kappa_3$. [g] Composition of sample uncertain; may contain $CH_3HgHBIm^+$.

The nonexponential phosphorescence decay observed at 77 K for each of the complexed species vitiates the use of the microwave saturated phosphorescence decay experiment[31,34,35] from which the individual sublevel $T_i \rightarrow S_0$ decay constants can be obtained when spin-lattice rates are not negligible. The MIDP method, however, is useful for obtaining the relative energy ordering of shorter lived, more radiative sublevels and the longer lived ones which are less radiative, provided that spin-lattice relaxation does not dominate sublevel decays. The quantitative lifetime data must be treated cautiously, however. The MIDP and microwave-induced phosphorescence transient[25] experiments proved to be difficult to evaluate quantitatively for the complexes $CH_3HgTrp$ and $CH_3HgTam^+$, since in each case, two sublevel decay constants proved to be very large. The maximum microwave sweep rate available with our apparatus is $2 \times 10^5$ MHz/s below 4 GHz, and $4 \times 10^5$ MHz/s between 4 and 8 GHz. Given the line widths of the transitions listed in Table III, a minimum of about 1 ms is required to accomplish a microwave passage through a signal. In the case of $CH_3HgTam^+$, each MIDP transient and microwave-induced phosphorescence transient signal at the maximum microwave sweep rate had the appearance of a slow passage signal, i.e., a symmetrical peak. For $CH_3HgTrp$, the $\nu_1$ and $\nu_3$ transitions also had this appearance. This behavior is consistent with microwave pumping of a sublevel whose decay lifetime is shorter than or of the same order as the microwave passage time. In the case of the $\nu_2$ transition of $CH_3HgTrp$, an average decay lifetime of the MIDP transient of ca. 4.1 ms was measured, which is considerably longer than the passage time through the signal, and was taken as an estimate of the decay lifetime of the longer lived of two short-lived sublevels. The amplitude of the MIDP transients decayed exponentially with a decay lifetime averaging 48 ms in $CH_3HgTrp$ and 33 ms in $CH_3HgTam^+$. These are taken as the estimated lifetimes of a single long-lived triplet sublevel in each complex. An estimate of the shortest sublevel lifetime was obtained by deconvolution of the pulsed laser excited phosphorescence decay at 1.1 K. For $CH_3HgTrp$, decay lifetimes of 48 and 4.1 ms were fixed in the analysis, and the total phosphorescence decay was fit to three exponential components. The deconvoluted decay was dominated (~80%) by a short component (0.38 ms) which is taken as the decay lifetime of the shortest lived sublevel. In the case of $CH_3HgTam^+$, only one component was fixed in the analysis (33 ms) and the phosphorescence decay was fit only to a total of two exponential components. The dominant (97%) component of the decay (0.48 ms) is taken as an average of two short sublevel decay lifetimes which probably are of comparable magnitude. For both $CH_3HgTrp$ and $CH_3HgTam^+$ the two shortest lived sublevels are connected by the $\nu_1$ transition, since the MIDP response amplitude was found to be very much weaker for this transition than for $\nu_2$ and $\nu_3$. If spin-lattice relaxation were completely absent, this MIDP signal would vanish completely after the populations of the two short-lived levels had decayed to zero. Since it was observed when exciting the $\nu_1$ transition, especially in $CH_3HgTam^+$ where the $\nu_1$ and $\nu_2$ transitions are completely resolved, we can assume that spin-lattice relaxation is not negligible in these complexes at 1.1 K. In $CH_3HgTrp$, we find that the sublevel with intermediate lifetime is intermediate in energy. Analysis of the MIDP experiments on the HBIm complexes was straightforward since the sublevel lifetimes are considerably longer and fast passage conditions could be achieved. Furthermore, spin-lattice relaxation effects are less important since MIDP was observed only when exciting the $\nu_2$ and $\nu_3$ transitions. The decay lifetime of the MIDP transient differed for $\nu_2$ and $\nu_3$, but the decay of the transient initial amplitude was found to be the same at both these frequencies within experimental error. This demonstrates that each complex has two short-lived sublevels, and that they are connected by the $\nu_1$ transition. The data for the MIDP and laser-excited phosphorescence decay measurements are given in Table IV.

**Table V.** Nuclear Magnetic Resonance Data for Methylmercury Protons in Several Complexes[a]

| complex | $\Delta\nu/\nu_0$, ppm[b] | $J(^1H-^{199}Hg)$, Hz |
|---|---|---|
| $CH_3HgOH$ | −3.94 | 203.0[c] |
| $(CH_3Hg)$ glycine | −3.92 | 215.5 |
| $CH_3HgTrp$ | −4.68 | *d* |
| $CH_3HgTam^+$ | −4.67 | 213.1 |
| $(CH_3Hg)HBIm^+$ | −3.68 | 218.4 |

[a] Measurements at room temperature in $D_2O$. pH 7–8, except $(CH_3Hg)HBIm^+$ for which pH 6.2. Amine concentration is in the range 5–10 mM and is in molar excess over added $CH_3HgOH$. Observed $\Delta\nu$ and $J$ corrected for partitioning of $CH_3Hg(II)$ between complex and $CH_3HgOH$ using data of Table I. [b] NMR frequency shift relative to HDO proton taken as 0.00. [c] Datum from ref 15. [d] $CH_3$ signal is broad. $^{199}Hg$ satellites not observed.

The methylmercury proton chemical shifts for the HTrp, $HTam^+$, and HBIm complexes and the $^{199}Hg-^1H$ spin-spin coupling constants are compared with those of $CH_3HgOH$ and the glycine complex in Table V. The $CH_3$ protons are subjected to a considerable downward frequency shift in $CH_3HgTrp$ and in $CH_3HgTam^+$ relative to the glycine complex. The frequency shift is upward in $CH_3HgHBIm^+$.

## Discussion

Methylmercury is observed to bind readily to HTrp, HBIm, and $HTam^+$. In Figure 4 we have made a plot of the amine $pK_a$ vs. log $K_f$ for the compounds listed in Table I, and have introduced a linear regression line for the primary aliphatic amines (including $NH_3$ and β-aminopropionic acid). There is a linear inverse correlation between $pK_a$ and log $K_f$ for these molecules, although the regression is determined only by the cluster of primary amines with $pK_a$ near 10.8, β-aminopropionic acid, and $NH_3$. The $K_f$ of glycine is about a factor of 3 larger than predicted by the regression, suggesting that a carboxylate group attached at the α-carbon atom enhances the binding of $CH_3Hg^+$ relative to proton binding. This effect has been noted previously by Rabenstein and co-workers,[15,36] who suggest the possibility of some degree of chelation in the glycine complex. This enhancement of $K_f$ is not present in valine, however, which falls near the regression line, possibly because the bulky isopropyl side chain reduces the interaction between $CH_3Hg^+$ and the carboxylate. The enhancement of $K_f$ is about a factor of 10 for $HTam^+$, and can be attributed to a specific interaction between the indole ring and $CH_3Hg^{II}$. The $K_f$ for tryptophan, however, is about 60 times that predicted by the regression, which is roughly of the magnitude expected if the interactions of $CH_3Hg^{II}$ with the indole ring and the carboxylate were additive in this complex. Finally, the stability of the phenylalanine complex is enhanced about 10-fold over that expected and indicates specific interaction of $CH_3Hg^{II}$ with the phenyl group.

The results of NMR measurements listed in Table V show that relative to the glycine complex, the $CH_3$ protons of $CH_3Hg^{II}$ experience a downward frequency shift of 0.75–0.76 ppm in the complexes $CH_3HgTam^+$ and $CH_3HgTrp$. In the complex $CH_3HgHBIm^+$ we find an upward frequency shift of 0.24 ppm. We believe that these shifts are due to ring current effects of the indole and benzimidazole rings, respectively. The shifts are in the directions expected if the $CH_3$ protons reside above the indole ring in $CH_3HgTam^+$ and $CH_3HgTrp$, and near the benzimidazole plane in $CH_3HgHBIm^+$. The latter geometry is expected intuitively for σ bonding of $CH_3Hg^{II}$ to N3 of HBIm. Rabenstein et al.[15] attributed their observed 0.5-ppm upfield shift (corresponding to a downward frequency shift at constant field) of the $CH_3Hg^{II}$ protons in the phenylalanine complex vs. the glycine complex to a ring current shift, and suggested that the methyl group lies close to and above the plane of the phenyl ring. We have made space-filling models of the aromatic amino acids and $HTam^+$ with $CH_3Hg^{II}$ replacing an aminium proton; we find in each case that the aliphatic side chain can readily assume an unstrained conformation which allows the $CH_3Hg^{II}$ to overlie the aromatic ring in close contact with the π system. Furthermore, it is not possible to bring the methyl group over the aromatic ring without also allowing close contact of the Hg atom with the π system. In the model, the C–Hg–N line is approximately parallel to the aromatic plane.

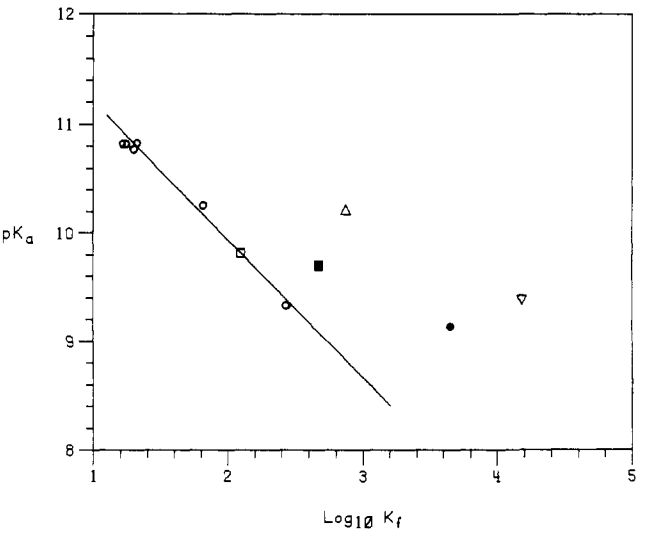


**Figure 4.** Primary amine $pK_a$ vs. log $K_f$ (defined by eq 1) for binding of methylmercury. Data are from Table I. ○, primary amines, β-aminopropionic acid, and ammonia; □, valine; ■, glycine; △, tryptamine; ●, phenylalanine; ▽, tryptophan. Regression line refers to the aliphatic primary amines, β-aminopropionic acid, and ammonia data points.

The models suggested by the NMR measurements for the $CH_3Hg^{II}$ complexes of HTrp, $HTam^+$, and HBIm account at least qualitatively for the different magnitudes of the heavy-atom effect as measured by the perturbed triplet state lifetimes. The similar triplet lifetimes found for $CH_3HgTrp$ and $CH_3HgTam^+$ suggest that the complexes are of the same type, in agreement with the NMR data. Unperturbed HBIm, $H_2BIm^+$, and $HTam^+$ have similar phosphorescence lifetimes which are in the range 6–7 s.[31,33] We attribute the striking difference in the perturbed triplet lifetimes of $CH_3HgTrp$ (and $CH_3HgTam^+$) vs. $CH_3HgHBIm^+$ (and $(CH_3Hg)_2BIm^+$) to the different geometrical relationship between the heavy-atom perturber and the triplet state chromophore. In the external heavy atom effect theory of Robinson,[37] the perturbed triplet state steals radiative intensity from a spin-forbidden transition which is considered to be relatively localized on the perturber (the Hg atom in our case). The extent of mixing of perturber triplet states varies directly with the magnitude of the exchange interaction between the triplet electron pair of the π system and the electrons associated with an excited triplet state of the perturber. Since we are dealing in each case with the same perturber and all other parameters in Robinson's theory are expected to be relatively invariant, we can associate the large difference between the extent of the heavy-atom perturbation of HBIm vs. HTrp (and $HTam^+$) with the difference in the exchange interaction. The latter is of short range and increases with overlap of the triplet state wave functions of molecule and perturber; we conclude that the overlap of orbitals associated with localized virtual excited states of Hg with the π orbitals associated with the aromatic ring must be significantly greater in the complexes $CH_3HgTrp$ and $CH_3HgTam^+$ than in $CH_3HgHBIm^+$. We believe that this qualitative conclusion supports the models for these complexes discussed earlier in connection with NMR results.

It may be noted from Table IV that the apparent triplet sublevel decay constants vary widely for a given complex. This implies that in these complexes the heavy atom effect is spin sublevel selective. It should be pointed out that the theory of the external heavy atom effect applies to enhancement of the *radiative* rate constants[18,37] and that the $\kappa_i$ of Table IV refer to apparent total decay constants which include the contributions of radiationless $T_i \rightarrow S_0$ processes and (probably to a lesser extent) spin-lattice relaxation. At least in the case of $CH_3HgTrp$, however, which has a large (~0.9) radiative phosphorescence quantum yield, $\kappa_3$ represents mainly a radiative decay constant. Thus, we see that in this case the heavy-atom perturbation is highly selective. Although no quantitative measurements of phosphorescence quantum yields were made for $CH_3HgTam^+$ and $CH_3HgHBIm^+$, qualitatively there occurs an enhancement of the phosphorescence yield upon complexing which accompanies the fluorescence quenching. We believe, therefore, that the dominant decay components of Table IV are reflective of radiative processes. Measurements of the relative radiative decay constants of the individual sublevels of the $CH_3Hg(II)$ complexes are in progress; these will lead to a more accurate assessment of the spin sublevel selectivity of the $CH_3Hg^{II}$ heavy atom effect and possibly to clues regarding the detailed electronic mechanism.

Protonation and complexing of HBIm with $CH_3Hg^{II}$ lead to large and virtually identical changes in the ZFS, characterized most obviously by a reduction of $|E|$. In the case of protonation, the resulting cation has $C_{2v}$ symmetry as a result of charge resonance between the equivalent structures Ia and Ib. The in-plane principal axes of the ZFS in this case are re-

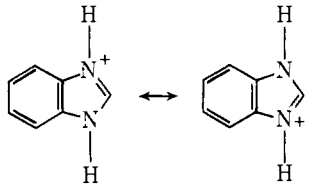

Ia Ib

stricted by symmetry to lie along, and perpendicular to, the twofold axis. We have previously[31] assigned the ZFS of this cation as $D = 11.80$, $E = -1.32\ m^{-1}$ on the basis of sublevel decay constant measurements and by analogy with $D$ and $E$ values known experimentally for analogous $^3(\pi,\pi^*)$ states. The assignment refers to the Hamiltonian,

$$\mathcal{H}_s = D(S_x^2 - 2/3) + E(S_z^2 - S_y^2)$$

with the principal $x$ axis normal to the plane, and $z$ along the twofold symmetry axis. In this assignment, the $\nu_1$ ODMR transition (Table III) occurs between the $T_y$ and $T_z$ sublevels, while $\nu_2$ and $\nu_3$ connect $T_x$ with $T_y$ and $T_z$, respectively. Based on the essentially identical values observed for the $\nu_i$ of $CH_3HgHBIm^+$ and of $(CH_3Hg)_2BIm^+$ we make the same assignment of $D$ and $E$ for these ions. It has been argued previously[38,39] that a localized double bond conjugated with a phenyl or pyrimidine ring, i.e., a single strongly mesomeric group, leads to the large value of $|E|$ observed in the triplet states of such molecules as indole, purine, and HBIm. Protonation of HBIm leads to the loss of the localized double bond of the imidazole ring as a result of the charge resonance between equivalent structures represented above (Ia ↔ Ib). Consequently, the reduction in $|E|$ upon protonation of HBIm follows from the previous arguments[38,39] regarding the effect of the mesomeric group on the ZFS of the triplet state. In the unsymmetrical ion $CH_3HgHBIm^+$, the reduction of $|E|$ by the amount corresponding to protonation implies that the structures IIa and IIb have approximately equal weight in the charge resonance. The complex $(CH_3Hg)_2BIm^+$ has $C_{2v}$

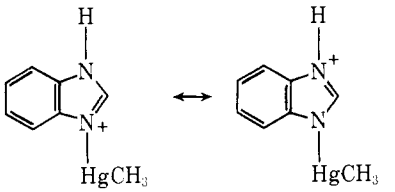

IIa IIb

symmetry, and should have $D$ and $E$ values similar to those of $H_2BIm^+$ if the effects of $CH_3Hg^{II}$ complexing are mimicked by protonation. Since $D$ and $|E|$ are observed to be virtually identical in $(CH_3Hg)_2BIm^+$ and $H_2BIm^+$, we can conclude that the effect of $CH_3Hg^{II}$ complexing on the ZFS of HBIm is the same as that of protonation. We can think of no reason why this conclusion should not be generally applicable to $^3(\pi,\pi^*)$ states of aromatic molecules; exceptions would be orbitally degenerate or nearly degenerate states where small electrostatic perturbations can cause large changes in electron distributions.

From the assignment of ZFS and the principal axis system of $CH_3HgHBIm^+$ and of $(CH_3Hg)_2BIm^+$, we find that the longest lived and therefore least perturbed sublevel is $T_x$. $T_y$ and $T_z$ have comparable apparent decay constants in these complexes, but any evaluation of the relative heavy atom effect on these sublevels is premature in the absence of data on the radiative rate constants.

The ZFS of HTrp and $HTam^+$ are nearly identical; $CH_3HgTrp$ and $CH_3HgTam^+$ differ considerably, however. One cannot rule out the influence of spin-orbit coupling on the ZFS in these complexes, since the heavy atom effect is considerably larger than it is in the HBIm complexes, where it is negligible. The NMR evidence suggests that $CH_3HgTrp$ and $CH_3HgTam^+$ have similar structures; also, their triplet lifetimes are similar. It is expected, therefore, that the effect of spin-orbit coupling in the two complexes would be similar, and not lead to large differences in the ZFS such as those observed. It is more probable that the differences in ZFS arise from electrostatic effects. The absence of a negatively charged carboxylate group in the vicinity of the indole ring in $CH_3HgTam^+$ would lead to a very different electrostatic perturbation than that of $CH_3HgTrp$; it would result in a different $\pi$-electron distribution, and, therefore, different ZFS based upon an electron spin-spin dipolar mechanism.[40]

**Acknowledgments.** We wish to thank Mr. Paul Bruins for running the NMR spectra. This work was partially supported jointly by the National Institute of Environmental Health Sciences, USPHS, and the U.S. Environmental Protection Agency.

## References and Notes

(1) J. M. Wood, *Adv. Environ. Sci. Technol.*, **2**, 39 (1971).
(2) F. Berglund and M. Berlin, "Chemical Fallout", M. W. Miller and G. C. Berg, Ed., Charles C. Thomas, Springfield, Ill., 1969.
(3) C. Ramel, *Hereditas*, **57**, 445 (1967); **61**, 208 (1969).
(4) C. Ramel and J. Magnusson, *Hereditas*, **61**, 231 (1969).
(5) G. Löfroth, "Methylmercury", Bulletin No. 4, Swedish Natural Science Research Council, Stockholm, 1969.
(6) J. J. Mulvihill, *Science*, **176**, 132 (1972).
(7) R. B. Simpson, *J. Am. Chem. Soc.*, **83**, 4711 (1961); **86**, 2059 (1964).
(8) R. Ferreira, E. Ben-Zvi, T. Yamane, J. Vasilevskis, and N. Davidson, in "Advances in the Chemistry of Coordination Compounds", S. Kirschner, Ed., Macmillan, New York, N.Y., 1961, p 457.
(9) D. W. Gruenwedel and N. Davidson, *J. Mol. Biol.*, **21**, 129 (1966); *Biopolymers*, **5**, 847 (1967).
(10) D. W. Gruenwedel and D. S. Lu, *Biochem. Biophys. Res. Commun.*, **40**, 542 (1970).
(11) D. W. Gruenwedel, *Eur. J. Biochem.*, **25**, 544 (1972).
(12) S. Mansy, T. E. Wood, J. C. Sprowles, and R. S. Tobias, *J. Am. Chem. Soc.*, **96**, 1762 (1974).
(13) S. Mansy and R. S. Tobias, *J. Am. Chem. Soc.*, **96**, 6874 (1974).
(14) S. Libich and D. L. Rabenstein, *Anal. Chem.*, **45**, 118 (1973); D. L. Rabenstein, C. A. Evans, M. C. Tburangeau, and M. T. Fairhurst, *Anal. Chem.*, **47**, 338 (1974).
(15) D. L. Rabenstein, R. Ozubko, S. Libich, C. A. Evans, M. T. Fairhurst, and C. Suvanprakorn, *J. Coord. Chem.*, **3**, 263 (1974).

(16) For a review, see A. L. Kwiram, *MTP Int. Rev. Sci.: Phys. Chem., Ser. One*, **4**, 271 (1972).
(17) M. Kasha, *J. Chem. Phys.*, **20**, 71 (1952).
(18) G. G. Giachino and D. R. Kearns, *J. Chem. Phys.*, **52**, 2964 (1970); **53**, 3886 (1970).
(19) K. F. S. Luk, R. J. Hoover, and A. H. Maki, *J. Am. Chem. Soc.*, **97**, 1241 (1975).
(20) R. R. Anderson and A. H. Maki, *Photochem. Photobiol.*, **25**, 585 (1977).
(21) T. D. Waugh, H. F. Walton, and J. A. Laswick, *J. Phys. Chem.*, **59**, 395 (1955).
(22) A. H. Maki and T.-t. Co, *Biochemistry*, **15**, 1229 (1976).
(23) J. Schmidt, D. Antheunis, and J. H. van der Waals, *Mol. Phys.*, **22**, 1 (1971).
(24) J. Zuclich, J. U. von Schütz, and A. H. Maki, *J. Am. Chem. Soc.*, **96**, 710 (1974).
(25) C. J. Winscom and A. H. Maki, *Chem. Phys. Lett.*, **12**, 264 (1971).
(26) G. Schwartzenbach and M. Schellenberg, *Helv. Chim. Acta*, **48**, 28 (1965).
(27) C. A. Evans, D. L. Rabenstein, G. Geier, and I. Erni, *J. Am. Chem. Soc.*, **99**, 8106 (1977).
(28) A. Albert in "Physical Methods in Heterocyclic Chemistry", Vol. I, A. R. Katritzky, Ed., Academic Press, New York, N.Y., 1963, p 1.
(29) F. Bishai, E. Kuntz, and L. Augenstein, *Biochim. Biophys. Acta*, **140**, 381 (1967).
(30) R. F. Chen, *Arch. Biochem. Biophys.*, **166**, 584 (1975).
(31) P. Svejda, R. R. Anderson, and A. H. Maki, *J. Am. Chem. Soc.*, preceding paper in this issue.
(32) J. Zuclich, *J. Chem. Phys.*, **52**, 3586 (1970).
(33) A. H. Maki and J. Zuclich, *Top. Curr. Chem.*, **54**, 115 (1975).
(34) J. Zuclich, J. U. von Schütz, and A. H. Maki, *Mol. Phys.*, **28**, 33 (1974).
(35) T.-t. Co, R. J. Hoover, and A. H. Maki, *Chem. Phys. Lett.*, **27**, 5 (1974).
(36) D. L. Rabenstein, *Acc. Chem. Res.*, **11**, 100 (1978).
(37) G. W. Robinson, *J. Chem. Phys.*, **46**, 572 (1967).
(38) E. Kochanski and A. Pullman, *Int. J. Quantum Chem.*, **3**, 1055 (1969).
(39) E. T. Harrigan and N. Hirota, *J. Am. Chem. Soc.*, **97**, 6647 (1975).
(40) S. P. McGlynn, T. Azumi, and M. Kinoshita, "Molecular Spectroscopy of the Triplet State", Prentice-Hall, Englewood Cliffs, N.J., 1969, Chapters 9 and 10.

# Picosecond Studies of the Fluorescence Probe Molecule 8-Anilino-1-naphthalenesulfonic Acid

**G. W. Robinson,* R. J. Robbins, G. R. Fleming, J. M. Morris, A. E. W. Knight, and R. J. S. Morrison**

*Contribution from the Department of Physical Chemistry, University of Melbourne, Parkville, Victoria, Australia 3052.* *Received October 17, 1977*

**Abstract:** Picosecond time-resolved fluorescence studies of 8-anilino-1-naphthalenesulfonic acid (ANS) have been carried out in a water–ethanol mixed-solvent system. Combined with quantum yield results, these data provide further insight into the nonradiative processes that can take place in this interesting fluorescence probe molecule. In a mixed solvent, the interchange of solvent molecules at the solvent shell level is slow compared with subnanosecond fluorescence decay, and thus excited-state equilibrium cannot be established. *Local* solvent relaxation around the excited-state molecule, on the other hand, has been found to occur on picosecond time scales for these solvents. No evidence was found for any unusually large interactions between the supposedly highly polar excited state of ANS and water (or ethanol) nor was there any propensity for 1:1 complex formation between excited ANS and either of these solvent molecules in this solvent system. Rather, a general "bulk solvent effect" is indicated by the data. Since photoionization is most likely the dominant nonradiative path in polar solvents, while intersystem crossing fills this role in nonpolar solvents, caution should be exercised in transferring conclusions for purely polar solvent systems, such as the one studied here, to nonpolar or to mixed polar–nonpolar solvent systems. The interpretation of results using ANS as a biological fluorescence probe molecule could be similarly affected.

## Introduction

Molecules with fluorescence spectra, quantum yields, and lifetimes that are sensitive to their environment have been used as probes for structure studies of biological macromolecules for many years.[1-3] Some of the most widely used molecules in this work are the anilinonaphthalenesulfonates (ANS) and related molecules. 1,8-ANS (8-anilino-1-naphthalenesulfonic acid) shows a dramatic decrease in fluorescence quantum yield when the solvent is changed from ethanol ($\phi_F = 0.4$) to water ($\phi_F = 0.003$).[4] Accompanying the decrease in fluorescence yield is a large red shift in the fluorescence emission maximum.[4,5] A number of different explanations of this huge solvent effect on the excited-state lifetime have been given.[2,6,7] Highly pertinent to this point is the suggestion by Fleming et al.[8] that the major nonradiative pathway in ANS may be one-photon ionization.

The study of ANS in *aqueous solvents* seems particularly relevant to biological probe studies, yet to our knowledge there have been no measurements of the fluorescence lifetimes of ANS and related molecules in such solvents, simply because of the subnanosecond time scales required. Consequently, discussions of the photophysics of aqueous ANS have up to now involved experimentally observable absorption and fluorescence maxima and quantum yields, rather than the rates of radiative and nonradiative decay of the excited state. In this paper we present fluorescence lifetime data for 1,8-ANS in a series of water–ethanol mixtures. These data are combined with quantum yield determinations to evaluate the changes in both radiative and nonradiative decay constants as to the solvent composition is varied. A discussion of the results then follows.

* To whom correspondence should be addressed at the Department of Chemistry, Texas Tech University, Lubbock, Texas 79409.

## Experimental Section

1,8-ANS obtained from Sigma was used as supplied. Spectroscopic grade ethanol (Merck) and triply distilled water were used as solvents. Absorption and emission spectra were measured on a Cary 17 spectrophotometer and a Perkin-Elmer MPF3 spectrofluorimeter, respectively. For quantum yield determinations, a quinine sulfate fluorescence standard ($10^{-5}$ M, 1 M $H_2SO_4$, $\phi_F = 0.546$) was used.[9] A quadratic correction for refractive index variation was applied.[10]

Fluorescence lifetimes were measured on two instruments. Subnanosecond lifetimes were measured using the third harmonic (351 nm) of a mode-locked neodymium phosphate glass laser for excitation. An Electro-Photonics Photochron II streak camera coupled to a Princeton Applied Research optical multichannel analyzer system was used as detector. The design and operation of this equipment has been described in detail in other publications.[11,12] Right-angle detection geometry was used. Polarization bias was eliminated by using

0002-7863/78/1500-7145$01.00/0 